

# Plastic flow of polypropylene (PP) and a PP-based blend

## Part 1 *Experimental determination of thermal activation parameters*

K. PORZUCEK\*, G. COULON, J. M. LEFEBVRE, B. ESCAIG

*Laboratoire de Structure et Propriétés de l'Etat Solide, Unité Associée au CNRS 234, Université des Sciences et Techniques de Lille Flandres-Artois, 59655 Villeneuve d'Ascq, France*

The compressive deformation at constant strain-rate of pure polypropylene (PP) and one of its blends with high-density polyethylene (HDPE) and an ethylene propylene rubber (EPR) has been investigated in the low temperature range  $77\text{ K} < T < 300\text{ K}$ . A careful determination of the stress relaxation behaviour at yield reveals the existence of critical temperatures which relate the deformation mechanisms to glass transition molecular mobilities. A self-consistent thermodynamic analysis is performed in order to characterize the thermally activated plasticity developed in these materials.

### 1. Introduction

Much attention has been given to the study of structure-mechanical properties relationships in polypropylene (PP) and PP-based blends. As an example, it has been shown that PP has a very poor low-temperature impact strength and that this property may be improved through the adjunction of a dispersed rubber phase. The rubber phase generally used is a copolymer of polyethylene and polypropylene such as poly(ethylene-co-propylene) (PEP), ethylene-propylene-diene terpolymer (EPDM), ethylene propylene random copolymer (EPR). Although the rubber addition enhances the impact resistance of PP, it also causes simultaneously a decrease of the flexural modulus. High-density polyethylene (HDPE) is often introduced as a third component in the blend in order to minimize this modulus loss.

The morphology of PP-blends has been widely investigated with special reference to dispersion, size and structure of the rubber particles. Observation techniques include optical, scanning and transmission electron microscopy [1–4]. A few studies have focused on the dynamic mechanical response of PP-based systems [5, 6], as well as on the effect of the rubber phase on tensile properties [7–9]. Little work has been devoted to the compressive behaviour of these materials; we may mention Friedrich [10] and Duckett and Zihlif [11] who reported observations of shear bands induced in PP by compression at low temperature.

There is still a lack of accurate characterization of non-elastic (or plastic) mechanical properties of PP- and PP-based blends. The present work is an attempt to relate the microstructural characteristics of these systems to their plastic compressive behaviour over a wide temperature range.

Previous papers [12–15] have shown that the plastic deformation of solid polymers can be successfully

investigated using concepts and experimental techniques issued from physical metallurgy. This “metallurgical approach” is based on the existence of mobile plasticity defects in the molecular chain arrangement, similar to dislocations in crystalline materials [16]. It consists in performing a thermodynamic analysis of the elementary thermally activated deformation event. The characteristic parameters of plastic flow, i.e. the Gibbs free energy,  $\Delta G_a$ , and the activation volume,  $V_a$ , can be readily measured and the deformation mechanisms responsible for plastic flow may thus be identified.

However, up to now, only single-phase materials have been studied in this framework, e.g. glassy thermoplastics such as atactic polystyrene (PS) and atactic polymethylmethacrylate (PMMA) [13, 14], or thermoset resins such as polyimide (PABM) and epoxy systems [17, 18].

In the present paper, we extend this analysis to a semi-crystalline PP and to a multi-phase PP-based system (PP/HDPE/EPR). The main concern of this work is to show the important role played by the glass transition phenomena in the yielding mechanisms of these materials. Critical temperatures, associated with the onset of molecular mobilities responsible for the glass transition behaviour of the different phases, are clearly in evidence for the first time.

The first section deals with the concepts of thermally activated yielding and with the activation parameter measurements.

### 2. Thermal activation analysis of plastic flow

#### 2.1. Basic concepts in terms of dislocation-like defects

Yielding of glassy polymers generally results in the formation of localized shear bands, the degree of heterogeneity of which is strongly dependent on the

\* Present address: NORSOLOR, Groupe ORKEM, Centre de Recherches Nord BP57 62670, Mazingarbe.

past thermomechanical history of the samples. At the tip of such deformed regions, the chain arrangement might be viewed as a number of molecular defects propagating the "plastic" strain forward. Shear bands, which clearly appear below the conventional yield stress, thus originate from the nucleation and growth of these defects (or shear nuclei) past a critical size. The defects have been described either at the elementary scale as kinks along molecular rods [19], or at a larger scale as Volterra or Somigliana dislocations [20, 21]. Their motion through the polymer bulk is limited in extent due to the lack of molecular periodicity; it results in repeated nucleation steps as the applied stress,  $\sigma$ , is increased, leading to profuse shearing, i.e. to the flow of the solid observed at the yield stress,  $\sigma_y$ . Along these lines, yielding in polymers is described as the thermally activated and stress-aided growth of these shear nuclei past an energy barrier,  $\Delta G_0$ , opposed by localized obstacles specified by chain stiffness and/or entanglement spacing [21].

Owing to the relatively long times needed for structural relaxations to occur in the glassy state ( $\tau_R \geq 10^2$  sec), the kinetics of the yield behaviour may be modelled by Boltzmann quasi-equilibrium thermodynamics. Indeed, it has been shown [14] that characteristic times,  $\tau_{def}$ , for the elementary deformation events are in the range of, or smaller than  $10^{-3}$  sec. As mentioned earlier, this thermodynamic analysis gives access to two characteristic features of the elementary mechanism: (i) the Gibbs free energy of activation,  $\Delta G_a$ , computed as the integral over the barrier of the increment of the thermodynamical potential of the system, and (ii) the activation volume,  $V_a$ , defined as the stress dependence of  $\Delta G_a$

$$V_a = - \left( \frac{\partial \Delta G_a}{\partial \sigma} \right)_{T,P,structure} \quad (1)$$

$V_a$  is directly related to the critical size,  $V_c$ , of the shear nucleus, i.e.  $V_a$  reflects the spatial extent of the zone where monomer units undergo coherent thermal fluctuations [16, 22].

In the case where the yield stress,  $\sigma_y$ , is controlled by a single thermally activated deformation mechanism, the macroscopic non-elastic strain rate obeys a simple Arrhenius law

$$\dot{\epsilon}_p = \dot{\epsilon}_0 (\sigma - \sigma_i, T) \exp [-\Delta G_a (\sigma - \sigma_i, T)/kT] \quad (2)$$

The pre-exponential factor,  $\dot{\epsilon}_0$ , contains the stress and temperature dependence of structure terms (density of active sites, nucleus size);  $\sigma_i$  holds for the internal stress which represents the long-range elastic interactions between plasticity defects, i.e.  $\sigma_i$  reflects the defects arrangement issued from the past thermomechanical history. As such, it is a sound assumption to take  $\sigma_i$  proportional to the shear modulus,  $\mu$ :  $\sigma_i = A\mu$ , where  $A$  is a structure factor depending only on the defect distribution, i.e. where the temperature dependence of  $\sigma_i$  only arises through that of  $\mu$ , as experiments clearly show. The so-called effective stress,  $(\sigma - \sigma_i)$ , is the thermally activated component of the flow stress,  $\sigma$ , which acts at a local scale on a shear nucleus.

## 2.2. Activation parameters measurements

In order to test the plastic strain-rate law introduced in Equation 2, we are basically concerned with the evaluation of the Gibbs free energy of activation,  $\Delta G_a(\sigma - \sigma_i, T)$ . The detailed procedures for the determination of this quantity have already been described in previous papers [12, 14, 16]. For the sake of clarity, we shall recall only the main steps.

The Gibbs free energy,  $\Delta G_a$ , can be obtained through two different routes.

(i) Assuming that the entropy change is mainly due to the temperature variation of the elastic response of the material during the activation event,  $\Delta G_a$  is expressed with a reduced number of experimental (i.e. non-adjustable) parameters: (a) the temperature dependence of the strain rate  $kT^2(\partial \ln \dot{\epsilon}_p/\partial T)_{\sigma,\sigma_i} = \Delta H_0$ , i.e. the operational activation enthalpy; (b) the stress dependence of the strain rate  $kT(\partial \ln \dot{\epsilon}_p/\partial \sigma)_{T,\sigma_i} = V_0$ , i.e. the operational activation volume; (c) the shear modulus and the yield stress,  $\mu$  and  $\sigma_y$ , respectively.

This yields the following expression for  $\Delta G_a$

$$\Delta G_a = \left( \Delta H_0 + \frac{T}{\mu} \frac{d\mu}{dT} V_0 \sigma_y \right) \left/ \left( 1 - \frac{T}{\mu} \frac{d\mu}{dT} \right) \right. \quad (3)$$

where  $\Delta H_0(T)$  may also be written [16]

$$\Delta H_0(T) = -TV_0 \left( \frac{\partial \sigma_y}{\partial T} \right)_{\dot{\epsilon}_p,\sigma_i} \quad (3a)$$

According to Equations 1 and 2,  $V_0$  may be written

$$V_0 = V_a + \left( \frac{\partial \ln \dot{\epsilon}_0}{\partial \sigma} \right)_{T,\sigma_i} \quad (4)$$

(ii) Assuming that  $\Delta G_a = F(\sigma)\mu(T)$  [12, 22] leads to the so-called "integration method" in which one introduces, in order to integrate Equation 1, a reduced variable  $\tau$  defined through

$$\tau(T) = \frac{\mu(0)}{\mu(T)} \sigma_y(T)$$

where  $\mu(0) = \mu$  at 0 K.

According to this method,  $\Delta G_a$  is expressed as

$$\Delta G_a = \frac{\mu(T)}{\mu(0)} \int_{\tau(T)}^{\tau(0)} V_0(\tau) d\tau \quad (5)$$

The self-consistence of the determination of the Gibbs free energy of activation requires that the two routes (Equations 3 and 5) yield identical values for  $\Delta G_a$ . This will be the case as long as the experimental quantity,  $V_0$ , has the physical meaning of an activation volume,  $V_a$ , i.e. in the temperature range where the pre-exponential term  $\dot{\epsilon}_0$  in Equation 2 is not stress dependent. By inverting the strain-rate law of Equation 2, it follows then that  $\Delta G_a = \alpha kT$ , where  $\alpha = \ln(\dot{\epsilon}_0/\dot{\epsilon}_p)$ . As a consequence, the observed linear variation of  $\Delta G_a$  with temperature indicates that the plastic flow is governed by a single thermally activated deformation mechanism, as postulated, for Equation 2 to be obeyed.

According to Equations 3 and 5, the calculation of  $\Delta G_a$  requires the knowledge of the temperature dependence of the elastic shear modulus  $\mu(T)$ . Because the elastic response of polymers is strongly frequency

dependent, the basic question arises of choosing the frequency at which the dynamic mechanical measurements should be performed. It has been shown that the temperature dependence of the shear modulus,  $\mu$ , should be taken at the frequency  $\nu_{\text{def}}$  of the elementary molecular mechanism responsible for the non-elastic behaviour [14]. In a constant strain-rate test,  $\nu_{\text{def}}$  can be easily evaluated from the  $\alpha$  value, i.e. from the slope of the curve  $\Delta G_a = \alpha kT$

$$\nu_{\text{def}} = \nu_N \exp(-\alpha) \quad (6)$$

$\nu_N \approx 0.1 \nu_D$  where  $\nu_D$  is the Debye frequency of the solid [12]. In practice,  $\nu_{\text{def}}$  is not known a priori and the determination of  $\Delta G_a$  starts by measuring  $\mu(T)$  at an arbitrary frequency,  $\nu_{\text{mod}}$ . An iterative procedure has been proposed to obtain thereafter a self-consistent agreement between  $\nu_{\text{mod}}$  and  $\nu_{\text{def}}$  [14].

Such a thermodynamic analysis of the flow stress has already been applied to several polymer materials. PS and PMMA [13, 14] have been found to deform, at constant strain rate, following two distinct modes, on both sides of a critical temperature,  $T_c$ . Below  $T_c$ , a single mechanism is acting, akin to the low-temperature dislocation glide observed in crystals; it is rate-controlling with a stress-dependent activation energy,  $\Delta G_a$ , and is strongly localized as deduced from the low, roughly constant, value of the experimental activation volume. Above  $T_c$ , the deformation behaviour is characterized by a constant activation energy, with the stress dependence mainly in the pre-exponential term,  $\dot{\epsilon}_0$ . It suggests a plasticity of diffusional type, based on molecular movements related to those responsible for the low temperature component of  $\beta$  secondary relaxation processes. In the case of a highly cross-linked PABM thermoset resin, for which no indication of sub- $T_g$  relaxation mobilities has been found by dynamic testing only a dislocation glide mode has been found for deformation, in the entire temperature range under investigation (from 150 K up to 460 K) [17].

The application of this analysis to PP and a PP-blend will be reviewed in the following sections.

### 3. Experimental procedure

#### 3.1. Materials

Polypropylene and the polypropylene-blend were both supplied by ATOCHEM (Centre d'Etude, de Recherche et de Développement de Serquigny, France). The PP is a pure homopolymer with an average molecular weight  $\bar{M}_n = 280\,000$ . The blend is a ternary polypropylene/high-density polyethylene/random ethylene propylene copolymer blend (PP/HDPE/EPR). The HDPE and EPR contents are 3.5% and 17.5% by weight, respectively. PP and PP-blend have been produced by injection moulding in the form of candle-shaped samples (30 mm diameter and 250 mm long).

SEM observations of the blend, after cryo-fracture and extraction of the EPR phase by hot heptane, have shown that HDPE and EPR combine to form a core-shell structure, where HDPE is totally embedded in the EPR inclusions [6]. Direct observations of the morphology of the PP-blend by transmission electron

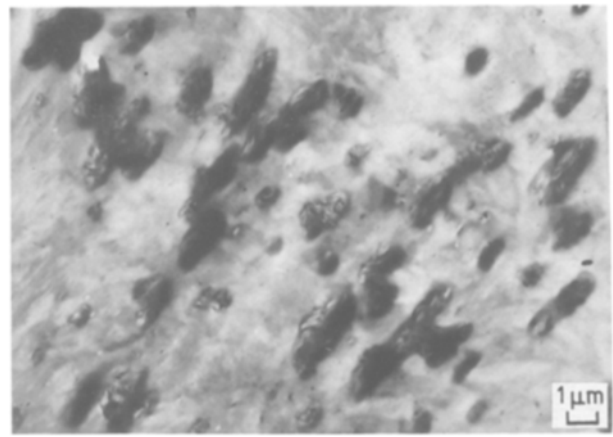


Figure 1 Morphology of the ternary PP/HDPE/EPR blend after THF/Zr staining and cryo-ultramicrotome sectioning.

microscopy (TEM) are difficult because of the poor contrast between the different phases. In addition, in order to enhance this contrast, it is impossible to use the well-known staining methods developed by Kato [23] and based on the osmium tetroxide ( $\text{OsO}_4$ ) reaction with carbon-carbon double bonds, because EPR is a saturated phase. Nevertheless, we have been able to produce a reasonable contrast of the rubber particles, using a heavy metal (zirconium) dissolved in tetrahydrofuran (THF) as a staining agent. Fig. 1 shows the typical TEM morphology of a cryo-ultramicrotomed thin section of PP/HDPE/EPR blend after such a treatment.

For compression testing, samples were machined in our laboratory into cylindrical specimens, 4 mm diameter and 9 mm long which were then mechanically polished to a length of 7.3 mm. The same isothermal annealing treatment (24 h at 393 K in air) was applied to each sample. The degree of crystallinity,  $\chi_c$ , as obtained from X-ray measurements, is equal to 57.5% and to 45.5% for PP and PP-blend, respectively [24].

#### 3.2. Deformation procedure

Uniaxial compression tests have been performed on an Instron machine at a constant applied strain rate  $\dot{\epsilon} = 4.5 \cdot 10^{-5} \text{ sec}^{-1}$ , in the temperature range  $77 \text{ K} < T < 293 \text{ K}$ . The experimental apparatus consists in a compact compression device conceived to ensure a perfectly guided uniaxial compression. This deformation apparatus is fitted into a liquid nitrogen cryostat. Temperature regulation is achieved with an accuracy of  $\pm 0.5 \text{ K}$ .

#### 3.3. Operational parameters measurements

The compressive yield stress,  $\sigma_y$ , is easily defined on the stress-strain ( $\sigma$ ,  $\epsilon$ ) curve. Whatever the temperature, the ( $\sigma$ ,  $\epsilon$ ) curves obtained for PP and for PP/HDPE/EPR blend exhibit a very distinct stress plateau (see Figs 2a and b). It has been shown that the corresponding stress value is precisely the yield stress  $\sigma_y$  [25].

The operational activation volume,  $V_0$ , is measured by a stress relaxation test at yield [16]. During this test, the stress drop,  $\Delta\sigma$ , is expressed as a function of time,

Figure 2 Stress-strain curves for (a) PP, (b) PP-blend.

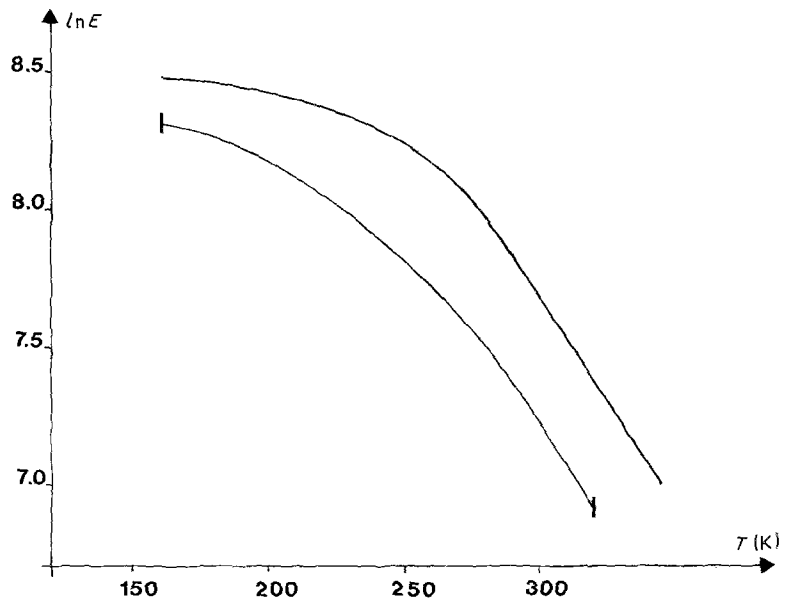
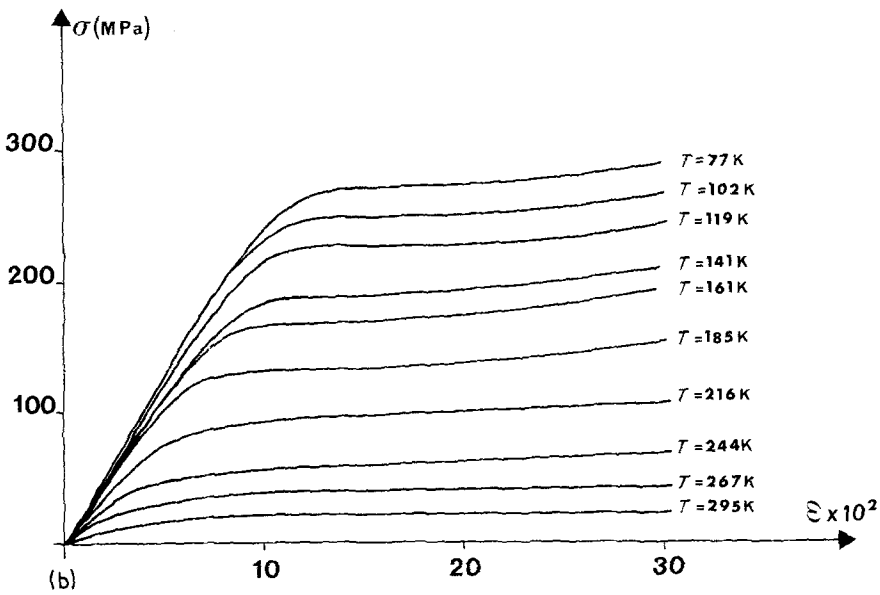
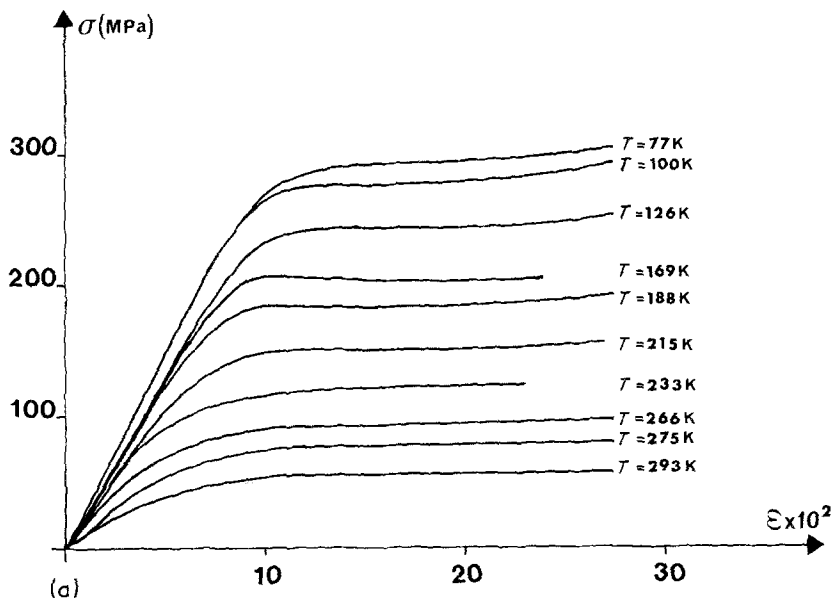


Figure 3 Logarithm of the Young modulus,  $E$  (MPa) plotted against temperature at  $10^2$  Hz: (—) PP; (---) PP-blend.

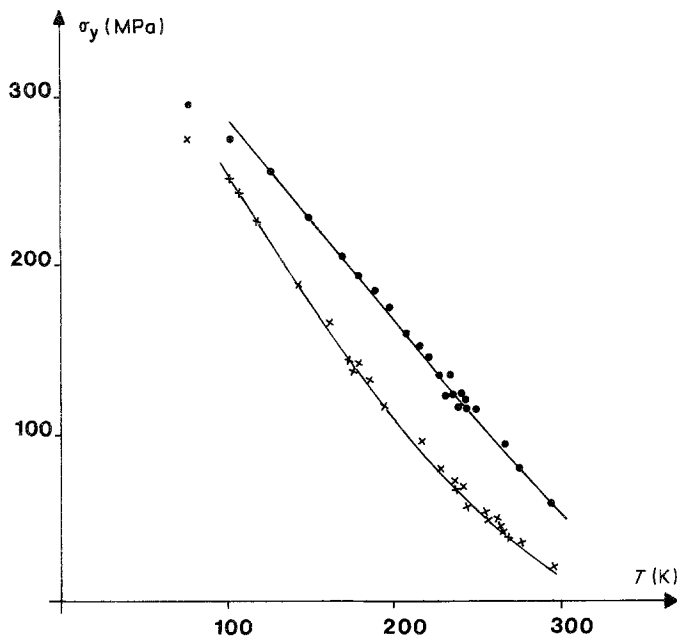


Figure 4 The temperature dependence of the yield stress: (●) PP; (x) PP-blend.

$t$ , in the following way [26]

$$\Delta\sigma(t) = \frac{kT}{V_0} \ln\left(\frac{t}{c} + 1\right)$$

where

$$c = \frac{kT}{MV_0\dot{\epsilon}_p} \quad (7)$$

$M$  is the elastic modulus of the sample-machine association,  $\dot{\epsilon}_p$  is the plastic strain rate at the beginning of the relaxation. A semi-log plot of  $\Delta\sigma$  against  $t$  yields the value of  $V_0$  in a straightforward manner.

Elastic modulus measurements were performed for frequencies varying from  $10^{-2}$  to  $10^3$  Hz. The low-frequency data ( $10^{-2}$ ,  $10^{-1}$ , 1 Hz) were obtained on a torsion pendulum, between 100 and 380 K [24]. Elastic moduli at 7.8 and  $10^3$  Hz were measured on a Metravib viscoelasticimeter in our laboratory, between 160 and 340 K. The measurements at  $10^3$  Hz are summarized in Fig. 3 in the form of  $\ln E$  against  $T$  plots. Note that the temperature variation of the Young modulus,  $E$ , is reported instead of that of the shear modulus,  $\mu$ . It has no influence on the results, because the quantity of interest in Equation 3 is the relative variation ( $1/\mu$ )( $d\mu/dT$ ).

#### 4. Results

The temperature dependence of the yield stress,  $\sigma_y$ , is reported in Fig. 4 for PP and for the blend. The strong decrease of  $\sigma_y$  with increasing temperature indicates that the propagation of plasticity defects is thermally activated. For example,  $\sigma_y$  decreases by a factor of 2 and 3 for PP and for the blend, respectively, when  $T$  is increased from 110 to 230 K. The yield stress of the blend is lower than that of PP, over the entire temperature range under investigation.

The values of the apparent activation volume,  $V_0$ , deduced from stress relaxation tests, are reported in Fig. 5 as a function of temperature for both materials. Three significant features are seen on these plots. These occur at

$$T_c \simeq 240 \text{ K for PP}$$

$$T_c' \simeq 175 \text{ K and } T_c'' \simeq 255 \text{ K, for the PP-blend}$$

The temperature variation of the operational activation enthalpy,  $\Delta H_0$ , as deduced from the data of Figs 4 and 5 according to Equation 3a, emphasizes these discontinuities (see Figs 6a and b). Further developments on these  $T_c$  temperatures will be given in a forthcoming paper.

The illustration of the determination of the Gibbs free energy of activation,  $\Delta G_a$ , as detailed in Part 2, is given in Fig. 6a in the case of PP; the elastic modulus has been measured at a frequency  $\nu_{\text{mod}} = 10^3$  Hz. The agreement between the two routes (Equations 3 and 5)

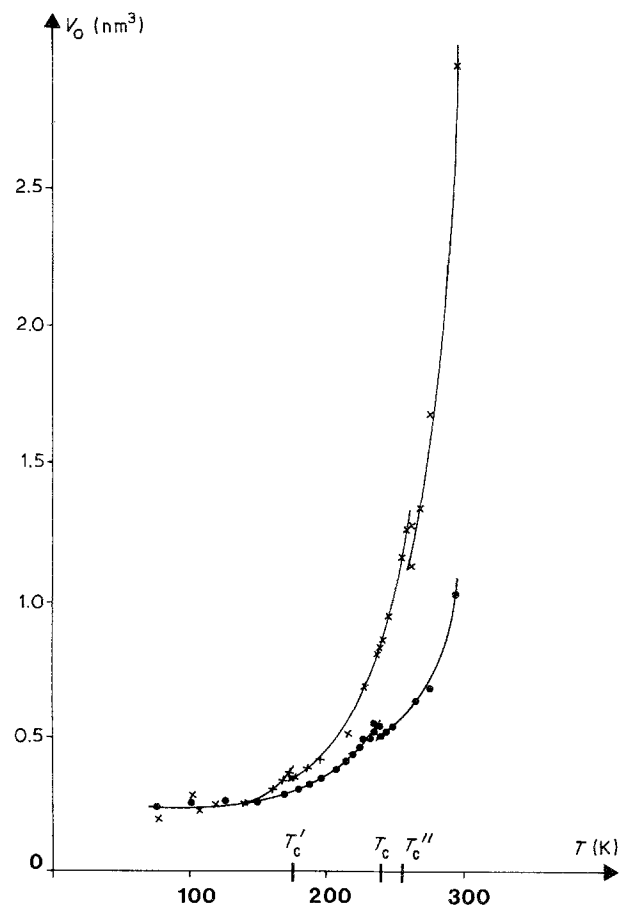


Figure 5 The temperature dependence of the operational activation volume,  $V_0$ : (●) PP; (x) PP-blend.

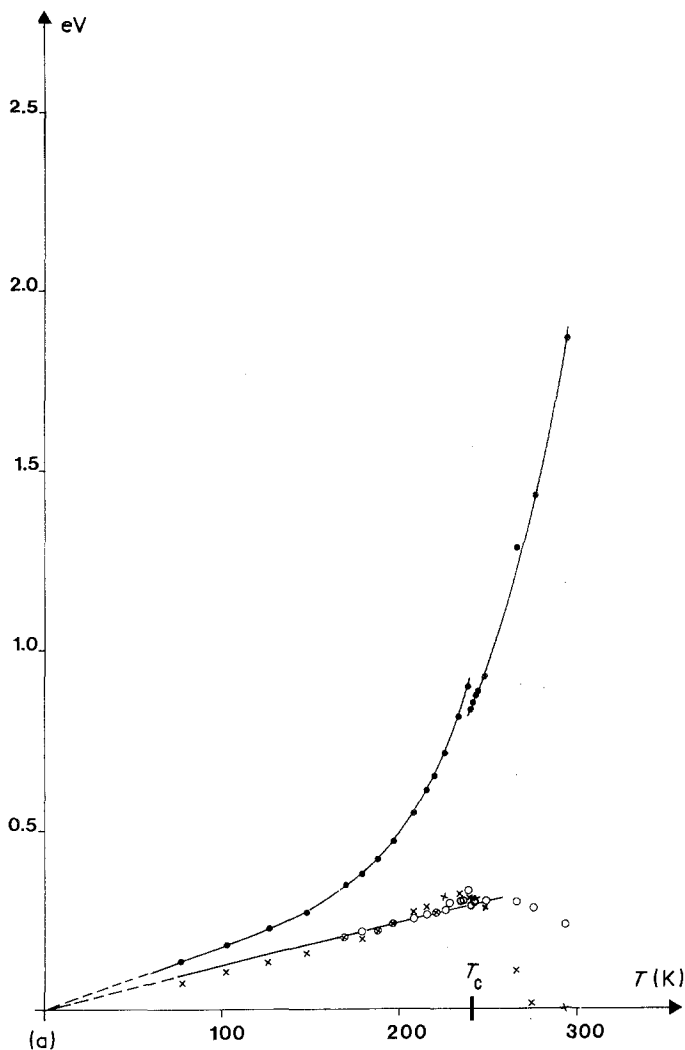


Figure 6 The temperature dependence of the operational activation enthalpy,  $\Delta H_0$  (●), and of the Gibbs free energy of activation,  $\Delta G_a$  (×) from Equation 3, (○) from Equation 5, (a) for PP, (b) for PP-blend.

is observed up to about 240 K. Consistently, below this temperature, the  $\Delta G_a(T)$  curve is a straight line going through the origin. Note that the comparison of  $\Delta H_0$  and  $\Delta G_a$  clearly confirms the large entropic contributions to the deformation process generally observed in polymer systems [13, 17, 18].

The same procedure has been applied to the PP-blend and yields the results in Fig. 6b. The self-consistent determination of  $\Delta G_a$  is there only valid up to around 175 K; in this range,  $\Delta G_a$  is again proportional to temperature. In both cases, i.e. for PP and its EPR blend, no conclusion may be drawn as soon as  $\Delta G_a$  values, derived from Equations 3 and 5, disagree. In other words, no meaningful information may be extracted regarding  $\Delta G_a$ , beyond 240 and 175 K for PP and the blend, respectively.

## 5. Discussion

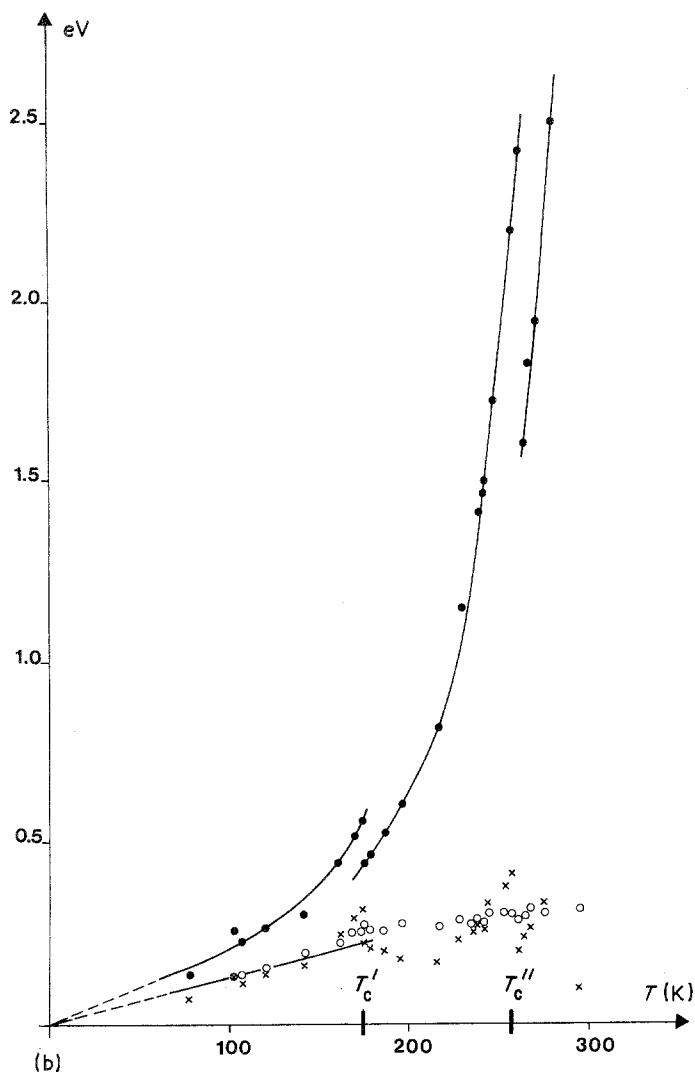
It is important to note that the following discussion is only concerned with the temperature range where the thermodynamic analysis provides relevant parameters of the deformation mechanisms involved at yield, i.e. for  $T < T_c \approx 240$  K in PP and for  $T < T'_c \approx 175$  K in the blend.

Through this thermodynamic and kinetic analysis of the plastic deformation behaviour, we have been able to check the assumption of a single thermally activated process. On one hand, the agreement between the two determinations of the Gibbs free energy of activation,  $\Delta G_a$ , indicates that, within the previous

temperature domains, the operational activation volume,  $V_0$ , has the physical meaning of a "true" activation volume,  $V_a$ , i.e.  $V_0$  is the stress derivative of the energy  $\Delta G_a$ . In other words, the pre-exponential factor,  $\dot{\epsilon}_0$ , introduced in Equation 2 is stress independent; the stress dependence of  $\dot{\epsilon}_p$  is thus predominantly exponential. On the other hand, the linear behaviour of  $\Delta G_a$  with temperature ( $\Delta G_a = \alpha kT$ ) confirms our assumption.

It is worth noting that for both materials one finds a similar slope  $\alpha \approx 14$ . The value of the elementary deformation frequency,  $\nu_{\text{def}}$ , as deduced from Equation 6, is thus equal to 830 kHz.  $\nu_{\text{def}}$  is clearly inconsistent with the frequency at which the elastic response was measured, i.e.  $\nu_{\text{mod}} = 1$  kHz. Owing to the lack of high-frequency dynamic mechanical techniques in our laboratory, we have not been able to apply the iterative method proposed in [14]. Nevertheless, it has been possible to deduce apparent values of  $\nu_{\text{def}}$  from  $\Delta G_a$  against  $T$  plots, for various low-frequency data (i.e. for  $\nu_{\text{mod}} = 10^{-2}, 10^{-1}, 1, 7.8$  and  $10^3$  Hz successively). As in the case illustrated in Figs 6a and b, the slope  $\alpha$  appears to be the same for PP and the blend whatever the frequency. The results are shown in Fig. 7 in the form of a log-log plot of  $\nu_{\text{def}}$  against  $\nu_{\text{mod}}$ , which can be fitted by a polynomial of degree 2. It is then straightforward to extrapolate the expected self-consistent value,  $\nu_{\text{def}}$ , from this curve:  $\nu_{\text{def}} \approx 85$  kHz.

The next step in the present analysis is to discuss the



molecular origin of the observed  $T_c$  temperatures. Fig. 8 gives the temperature dependence of the loss tangent,  $\text{tg } \delta$ , measured at  $\nu_{\text{mod}} = 1 \text{ kHz}$  for both materials. Although this frequency is lower than the value of  $\nu_{\text{def}}$ , we can see that  $T_c$  relates to the onset of molecular mobilities responsible for the glass transition in PP. In the same way,  $T_c'$  is associated with the  $T_g$  of the EPR phase.  $T_c''$ , also shown on the  $V_0(t)$  plot in the blend, is related to the glass transition of the amorphous PP phase.

Let us now return to the low-temperature thermally

activated deformation mechanism. As seen in Fig. 5, below  $\approx 150 \text{ K}$ , the operational activation volume,  $V_0$ , remains roughly constant and has the same value for both polymer systems. This common value of  $V_0$  is identified as the "true" activation volume,  $V_a$ , and has the physical meaning of the critical size  $V_c$  of shear nuclei undergoing a successful activation event.  $V_a = V_c \approx 0.5 \text{ nm}^3$ , once resolved in the shear plane, represents about six PP monomer units. This result proves the strong localization of the deformation event. As a comparison,  $V_c$  corresponds to the volume

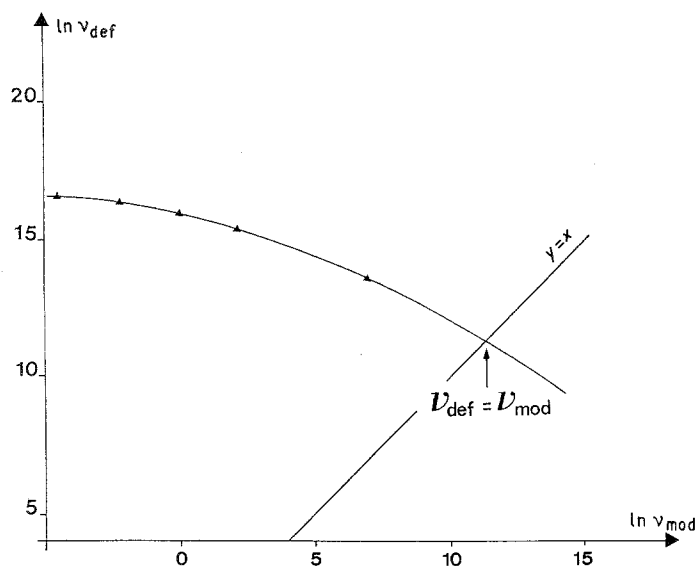


Figure 7 Common log-log plot of  $\nu_{\text{def}}$  against  $\nu_{\text{mod}}$  for PP and PP-blend.

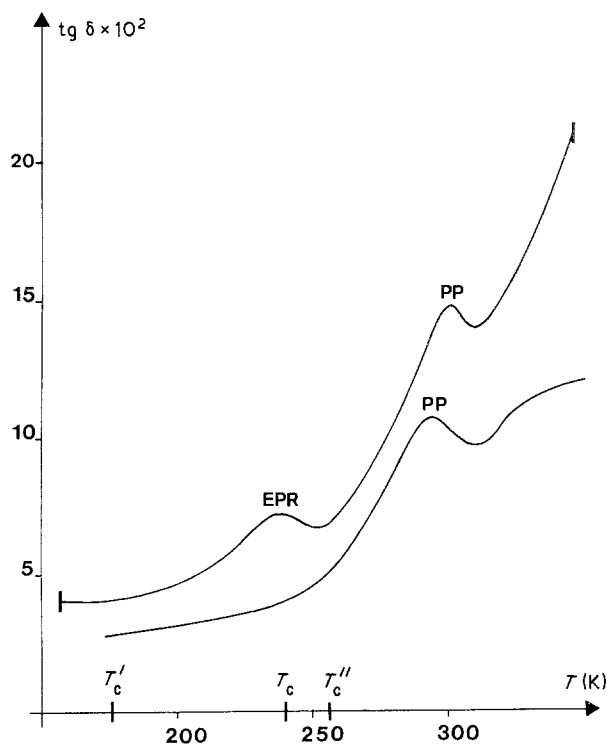


Figure 8 The temperature dependence of the loss tangent,  $\text{tg } \delta$ , at  $10^3$  Hz: (—) PP; (---) PP-blend.

of five or six monomer units for PS, less than two for PMMA, two or three for PEMA [27].

Although we are looking at semi-crystalline systems, we refer here to the nucleation of a plastic zone in the amorphous phase as being the rate-controlling process. Indeed, yielding should be far more difficult in the amorphous phase (owing to the lack of crystalline periodicity) than in the crystal lamellae. As a consequence, the similarity in plastic behaviour between PP and its blend, for temperatures lower than the  $T_g$  of the EPR phase, is not surprising because we are dealing in that case with equivalent glassy materials.

The following questions have not yet been addressed.

1. Does the appearance of a rubbery phase in the blend lead to a change in the local obstacle which controls yielding?

2. Alternatively, does it affect the long range internal stress field acting on the dislocation-like defects propagating plasticity?

A complementary approach, proposed in Part 2 of this paper, will allow us to answer these questions.

### Acknowledgements

Financial support under Contract M.I.R. 84-P-0719 is

gratefully acknowledged. K. Porzucek also thanks ATOCHEM for providing a doctorate research fellowship during the course of this work. The authors are indebted to C. Jourdan and J. Y. Cavaille for supplying results from [24].

### References

1. F. C. STEHLING, T. HUFF, C. S. SPEED and G. WISSLER, *J. Appl. Polym. Sci.* **26** (1981) 2693.
2. J. KARGER-KOCSIS, A. KALLO, A. SZAFNER, G. BODOR and Zs. SENYEI, *Polymer* **20** (1979) 37.
3. W. M. SPERI and G. R. PATRICK, *Polym. Engng Sci.* **15** (1975) 9.
4. J. KARGER-KOCSIS, L. KISS and V. N. KULEZNEV, *Polym. Commun.* **25** (1984) 122.
5. J. KARGER-KOCSIS, L. KISS and V. N. KULEZNEV, *Acta Polym.* **33** (1982) 14.
6. C. JOURDAN, J. Y. CAVAILLE, M. GLOTIN and J. F. PIERSON, Int. Symposium on Polymers for advanced technology IUPAC Symposium Proceedings, Jerusalem, 1987.
7. L. D'ORAZIO, R. GRECO, E. MARTUSCELLI and G. RAGOSTA, *Polym. Engng Sci.* **23** (1983) 489.
8. B. Z. JANG, D. R. UHLMANN and J. B. VAN DER SANDE, *ibid.* **25** (1985) 643.
9. M. KOJIMA, *J. Macromol. Sci. Phys.* **19** (1981) 523.
10. K. FRIEDRICH, *J. Mater. Sci. Letts.* **15** (1980) 258.
11. R. A. DUCKETT and A. M. ZIHLIF, *ibid.* **9** (1974) 171.
12. B. ESCAIG and J. M. LEFEBVRE, *Rev. Phys. Appl.* **13** (1978) 285.
13. J. P. CAVROT, J. HAUSSY, J. M. LEFEBVRE and B. ESCAIG, *Mater. Sci. Engng* **36** (1978) 95.
14. J. M. LEFEBVRE and B. ESCAIG, *J. Mater. Sci.* **20** (1985) 438.
15. G. COULON, J. M. LEFEBVRE and B. ESCAIG, *ibid.* **21** (1986) 2059.
16. B. ESCAIG, in "Plastic deformation of amorphous and semi-crystalline materials", edited by B. Escaig and C. G'sell (Les Editions de Physique, Les Ulis, 1982) p. 187.
17. J. M. LEFEBVRE, G. COULON, C. BULTEL and B. ESCAIG, *Mater. Sci. Engng* **84** (1986) 17.
18. X. CAUX, G. COULON and B. ESCAIG, *Polymer* **29** (1988) 808.
19. A. ARGON, *Phil. Mag.* **28** (1979) 839.
20. J. C. M. LI, in "Metallic glasses" (ASM, Metals Park, Ohio, 1978) p. 224.
21. B. ESCAIG, *Polym. Engng Sci.* **24** (1984) 737.
22. M. CAGNON, in "Dislocation et déformation plastique" (Les Editions de Physique, Les Ulis 1979) p. 53.
23. K. KATO, *Polym. Lett.* **4** (1966) 35.
24. C. JOURDAN, Thèse de l'INSA de Lyon (1987).
25. K. PORZUCEK, Thèse de l'Université de Lille I (1988).
26. F. GUIU and P. L. PRATT, *Phys. Status Solidi* **6** (1964) 111.
27. J. M. LEFEBVRE, Thèse de doctorat ès Sciences Physiques, Université de Lille I (1982).

Received 7 April

and accepted 5 September 1988